Geophysical Research Letters

RESEARCH LETTER
10.1029/2022GL101951

A Rapid Intensification Warning Index for Tropical Cyclones Based on the Analog Method

Deyu Lu[1,2], Ruiqiang Ding[3], Quanjia Zhong[1], Jiangyu Mao[1], Qian Zou[1,2], and Jianping Li[4,5]

[1]State Key Laboratory of Numerical Modeling for Atmospheric Sciences and Geophysical Fluid Dynamics (LASG), Institute of Atmospheric Physics, Chinese Academy of Sciences, Beijing, China, [2]College of Earth Science, University of Chinese Academy of Sciences, Beijing, China, [3]State Key Laboratory of Earth Surface Processes and Resource Ecology, Beijing Normal University, Beijing, China, [4]Key Laboratory of Physical Oceanography-Institute for Advanced Ocean Studies, Qingdao National Laboratory for Marine Science and Technology, Ocean University of China, Qingdao, China, [5]Laoshan Laboratory, Qingdao, China

Key Points:

- By using the information of tropical cyclones (TCs) early stage, a rapid intensification warning index (RIWI) is constructed based on the analog method
- The RIWI can distinguish between rapid intensification (RI) and non-RI storms during the early stages of TCs
- There is a significant positive correlation between a TC's RIWI and its lifetime maximum intensity

Supporting Information:

Supporting Information may be found in the online version of this article.

Correspondence to:

Q. Zhong,
zqj@lasg.iap.ac.cn

Citation:

Lu, D., Ding, R., Zhong, Q., Mao, J., Zou, Q., & Li, J. (2023). A rapid intensification warning index for tropical cyclones based on the analog method. *Geophysical Research Letters*, *50*, e2022GL101951. https://doi.org/10.1029/2022GL101951

Received 6 NOV 2022
Accepted 4 FEB 2023

Author Contributions:

Conceptualization: Deyu Lu, Ruiqiang Ding
Data curation: Deyu Lu
Formal analysis: Deyu Lu
Funding acquisition: Ruiqiang Ding
Investigation: Deyu Lu
Methodology: Deyu Lu, Ruiqiang Ding, Jianping Li
Project Administration: Ruiqiang Ding
Software: Deyu Lu
Supervision: Ruiqiang Ding, Quanjia Zhong, Jiangyu Mao, Qian Zou
Validation: Deyu Lu, Quanjia Zhong, Jiangyu Mao
Visualization: Deyu Lu
Writing – original draft: Deyu Lu

Abstract Prediction of the rapid intensification (RI) of tropical cyclones (TCs) remains challenging. In this paper, by using information from the early period following TC formation, the rapid intensification warning index (RIWI) is developed based on the analog method. A 10-year cross-validation and data from Hurricane Ida (2021) are used to verify its potential application. Results show that the RIWI can efficiently discriminate between RI and non-RI storms and has a significant positive correlation with the lifetime maximum intensity (LMI) of the TCs. By using this index, an early warning can be issued ~30 hr before the onset of RI, which is much earlier than the predictions made using the probabilistic Statistical Hurricane Intensity Prediction System RI index. In addition, by using the RIWI as a predictor, the prediction of LMI provides an early estimate of TC severity.

Plain Language Summary Variations in the intensity of tropical cyclones (TCs) are difficult to forecast, especially the occasional TCs that develop quickly over a period of couple of days; that is, rapid intensification (RI). Recent studies have demonstrated that it is easier to forecast RI likelihood than RI timing. Thus, instead of attempting to forecast the exact timing of RI, it may be more useful to predict whether RI will occur during the lifetime of a TC. In this paper, by using information from the early stage of TCs, we use the analog method to develop the RI warning index (RIWI). Then, using an appropriate threshold, it can be used to predict whether RI will occur during the lifetime of a TC. Furthermore, an important TC parameter, the lifetime maximum intensity (LMI) of the TC, has a significant positive correlation with its RIWI. The application of RIWI to Hurricane Ida (2021) is also presented in this paper and shows that an early warning can be issued ~30 hr before the onset of RI.

1. Introduction

Tropical cyclones (TCs) are one of the most destructive natural hazards and have had serious impacts in many countries (Emanuel, 2005; Needham et al., 2015). Storms that undergo periods of rapid intensification (RI; defined as the 95th percentile of 24-hr intensity changes) often lead to greater destruction because most go on to reach major hurricane status (wind speeds greater than 95 knots, categories 3–5 on the Saffir–Simpson scale; Lee et al., 2016). However, due to the deficiencies within the forecasting models, imperfect initial conditions, and limited intrinsic predictability, the prediction of RI has remained a substantial challenge over recent years (Blake et al., 2016).

Although great efforts have been made to decrease the errors associated with RI forecasting in numerical weather prediction (NWP; e.g., Emanuel & Zhang, 2016; Feng & Wang, 2019; Gall et al., 2013), the current operational models rarely generate accurate predictions of RI (Cangialosi et al., 2020). A case study explored by Judt and Chen (2016) indicated that the uncertainty associated with the prediction of the likelihood of RI occurrence is less than that associated with the prediction of RI timing, because the former is determined mainly by the TC environment. Hence, as a complement to NWP, many statistical approaches have been developed for the probabilistic prediction of RI instead of the deterministic prediction of RI. For instance, Kaplan and DeMaria (2003) developed a simple technique called the Rapid Intensification Index (RII), which uses five predictors to estimate the probability of RI. This method makes use of a combination of large-scale predictors and is used in RI prediction for TCs that develop over the Atlantic and the eastern and central North Pacific, which has been added to the

Writing – review & editing: Deyu Lu, Ruiqiang Ding, Quanjia Zhong

Statistical Hurricane Intensity Prediction Scheme (SHIPS) (Kaplan et al., 2010, 2015). Similarly, the SHIPS has been also developed for RI prediction in the western North Pacific (Shu et al., 2012). In general, the probabilistic prediction of RI has been improved to an extent by the above approaches, but more than half of RI events remain unpredictable within the 12–36 hr forecast period (Cangialosi et al., 2020).

There are a number of differences that distinguish RI hurricanes from non-RI hurricanes, such as sea surface temperature, eyewall contraction, and wind shear (e.g., Zhang & Sippel, 2009; Zhang & Tao, 2013). By considering these significant differences between RI and non-RI storms in the entire historical sample, the probability of RI is estimated by the above methods. However, as highly episodic and isolated events, RI hurricanes are not associated with one particular mechanism (Judt & Chen, 2016). For example, there are different eyewall formation processes during the RI period (Chen & Wu, 2022). For a certain TC, therefore, it may be more efficient to estimate the probability of RI in the analogous sample instead of in the entire historical sample. Moreover, the probabilistic forecasts using the above methods are generally skillful when multiple variables are used, whereas it has nearly no predictive skill when an individual variable is considered (e.g., DeMaria & Kaplan, 1994; Kaplan & DeMaria, 2003). To address these limitations, a new statistical method for estimating the likelihood of RI based on the analog method will be introduced in this paper. By identifying analogs in historical data, we developed the RI warning index (RIWI) to distinguish between RI and non-RI storms during the early stage of TC development, so that an early warning of RI can be issued when the RIWI reaches a certain threshold. In addition, the lifetime maximum intensity (LMI), an important statistic associated with TC intensification, shows a significant positive correlation with the RIWI.

2. Data and Methodology

2.1. Observational Data

The best track data set for TCs that developed over the Northern Atlantic (NA) basin over the period 1851–2019 was obtained from the International Best Track Archive for Climate Stewardship (IBTrACS) data set (Knapp et al., 2010, 2018). The NA Basin is defined as the region including much of the North Atlantic Ocean, the Caribbean Sea, the Gulf of Mexico, and a substantial portion of the adjacent coastal area. A case study of Hurricane Ida (2021), which was generated in the NA Basin, forms part of this study. To obtain the real-time RIWI for Hurricane Ida, we used the maximum surface winds (MSW) from the National Centers for Environmental Prediction (NCEP) Global Forecast System Final Analysis (GFS-FNL) data set. For comparison purposes, the performance of RII from SHIPS was also evaluated. The RII was available from the NHC official forecasts (Landsea & Franklin, 2013).

2.2. Analog Method

Analog forecasting is a method that has been widely used for TC intensity prediction (Lewis et al., 2020; Tsai & Elsberry, 2019). In this paper, the analog selection scheme used was the local dynamical analog (LDA) approach, which has been used to investigate atmospheric predictability (Ding et al., 2010, 2011; Li & Ding, 2011) and to correct model forecast errors (Hou et al., 2020). Following Zhong, Li, et al. (2018) and Zhong, Zhang, et al. (2018), we used the LDA method to find events similar to our TC of interest by considering the smallest sum of initial and evolutionary intensity errors. More details of how we found these analogous TCs are given in Supporting Information S1 (Figure S1).

3. Rapid Intensification Warning Index (RIWI)

3.1. Definition of the RIWI

By continuously searching for analogous hurricanes, we developed a new RI warning index (RIWI) that can generate an early warning prior to the onset of RI. Specifically, we used three steps to construct the RIWI (Figure 1).

Step 1. All analogous events for a certain time t_0 are identified using the LDA method (introduced in Section 2.2). Here, the analogous events are defined such that the difference in intensity variation between two events is relatively small (i.e., less than a minor value δ) over a short interval (m).

Step 2. As Figure 1 shows, we used the MSW to identify analogous hurricanes in this study. T_0 is the initial point of the time series. T_{0+m} is the start time of the search for analogous events. T_E is the end point for the

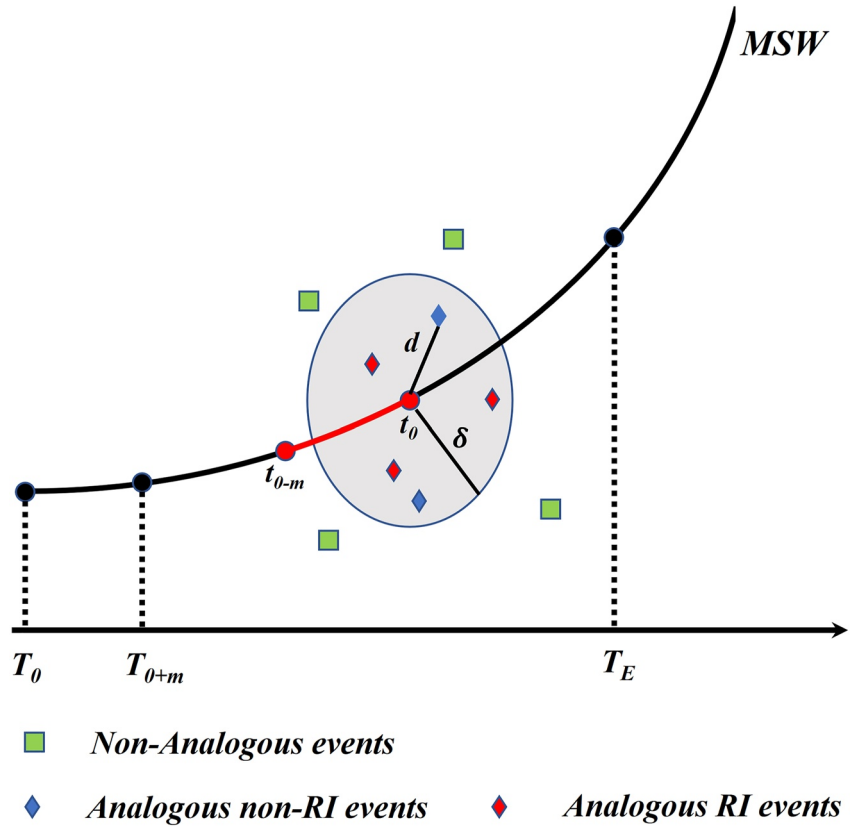

Figure 1. Schematic representation of the approach used in this paper. The analogous events were identified based on their MSW values. T_0 is the initial point of the time series. T_{0+m} is the start time for finding analogous events. T_E marks the end point of the search for analogous events. For a certain time t_0, d represents the LDA distance. $\boldsymbol{\delta}$ represents the distance threshold for searching for analogous points. If all points of an event are not analogous to t_0 (d is larger than $\boldsymbol{\delta}$), then the event is not similar to point t_0 and is represented by a green square. In contrast, the analogous events are represented by a rhombus. The non-RI events of the analogous events are blue, and the RI events are red. There is an evolution time (m) for the LDA method. For a certain time t_0, the period from t_{0-m} to t_0 is considered to get the LDA distance (represented by a red line).

search. The first step was repeated during the period from T_{0+m} to T_E. During this period, all analogous events are taken into account, which maximizes the number of similar events identified. Then, they are further classified as analogous RI events and analogous non-RI events.

Step 3. The TCs are classified into one of three types (i.e., non-analogous, analogous RI, and analogous non-RI events), and the RIWI is defined as the ratio of analogous RI events to all analogous events, which is given by:

$$\text{RIWI} = \frac{\text{Analogous RI events}}{\text{All analogous events}} \times 100\% \quad (1)$$

The three parameters used in this approach (m, δ, and T_E) were not randomly tested and determined. The settings for the parameter δ, m, and T_E were related to the standard deviation, the persistence, and the mean RI time following TC formation of the data, respectively. More detailed information is available in Supporting Information S1 (Text S1; Figure S2). In this paper, we took "m" to be 9 hr, δ to be five knots and T_E to be 63 hr, and the ability of the RIWI to distinguish between RI storms and non-RI storms was not sensitive to these three parameters within a certain range (Figure S2 in Supporting Information S1).

3.2. Characteristics of the RIWI Over the NA

The RI threshold is commonly defined as a change in MSW of 30 knots (15.4 m/s) over a 24 hr period (Kaplan & DeMaria, 2003). Using this threshold, we first calculated the RIWI for all TCs generated in the NA during

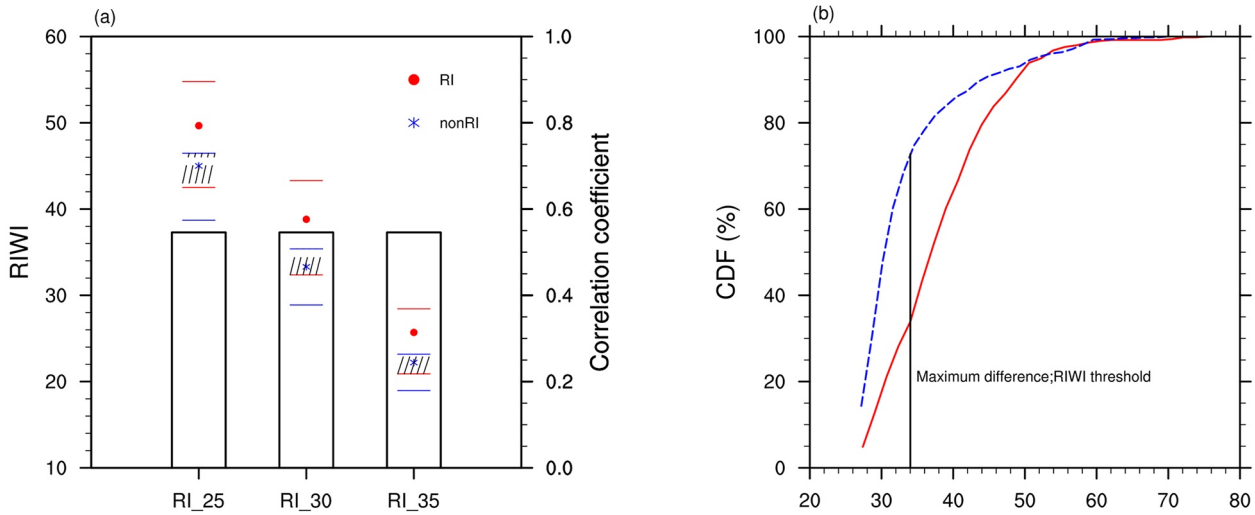

Figure 2. (a) The red dots and lines represent the average and the upper and lower quartiles of the RIWI for all RI events, respectively. The blue asterisks and lines represent the average and the upper and lower quartiles of RIWI for all non-RI events. The bar represents the correlation coefficient between RIWI and LMI for all events. The three distinct RI thresholds (i.e., 25, 30, and 35 knots) are shown separately in this figure. (b) The cumulative distribution functions of RIWI (RI threshold: 30 knots) for all RI events (red solid line) and non-RI events (blue dotted line). The black line represents the RIWI threshold for RI predicting, which is the maximum difference between two CDF lines.

our study period (1851–2019). The average RIWI values for RI and non-RI events were calculated separately. Furthermore, to investigate the impacts of different RI thresholds, two other RI thresholds (25 and 35 knots) were also used to calculate the RIWI. Although the RIWI values calculated using these three thresholds differed, all were able to distinguish RI events from non-RI events at a significance level of 0.05 (Figure 2a). In addition, the uncertainties of the MSW could lead to the uncertainties of the RIWI, which is represented by the upper and lower quartiles of RI storms (long red lines) and non-RI storms (long blue lines; Figure 2a). As we can see, the distributions of two kinds of storms cannot completely separate from each other (the shadow region in Figure 2a), indicating that there is no perfect selection criterion for RI predicting. Hence, to optimize selection of the RIWI threshold, an objective selecting method is introduced. As shown in Figure 2b, the cumulative distribution functions (CDF) of RIWI for RI storms and non-RI storms are represented by red solid line and blue dotted line, respectively. As the RIWI grows, the growth rates of CDF for two kinds of storms are different. Hence, to distinguish RI storms and non-RI storms as much as possible, the value of the RIWI with the maximum difference between the two CDF lines is determined as the selection of the RIWI threshold.

The LMI is an important statistic associated with TC intensification and reflects the severity of a TC (Emanuel, 2000; Kossin et al., 2014). Given that the bimodal nature of the LMI distribution reflects RI and non-RI hurricanes (Lee et al., 2016), the relationship between the LMI of a TC and its RIWI was also considered. The relationships for the three RI thresholds are summarized in Figure 2a and show positive correlations at a significance level of 99%. On the one hand, the RIWI only provides early information regarding the TCs, which is controlled mainly by initial errors and environmental conditions (Emanuel & Zhang, 2016). This significant positive correlation indicates that the LMI of TCs could be affected by their initial errors and environmental conditions. On the other hand, it also suggests that the RIWI could be regarded as a predictor for LMI forecasting. To test this hypothesis, we constructed three simple linear regression models to predict the LMI (Figure S3 in Supporting Information S1). The performance of these models is discussed in Section 4.

3.3. Verification of the RIWI Over the NA

The aforementioned results are based on the observational MSW data from 1851 to 2019. To explore how the RIWI performs in an independent data set, the total data set is often divided to the training set and testing set (Figure S4 in Supporting Information S1). However, this traditional method reduces the number of samples for the training set, which may cause overfitting and the selection bias (Wilks, 2006). Hence, the cross validation (Leave-one-out Cross validation) method was used in this paper. A comparison of these two methods could be

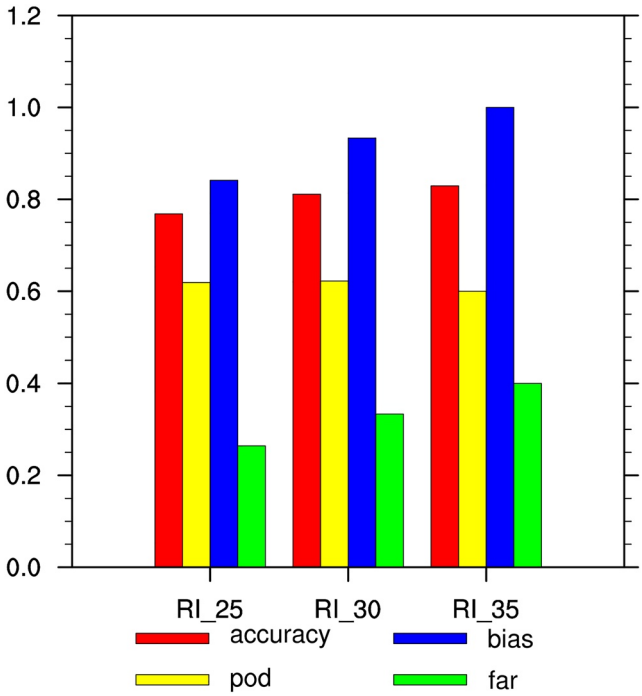

Figure 3. Cross-validation results for the 10-year period 2010–2019 were used to verify the early warning ability of the RIWI. Four scores were used: Accuracy (red), POD (yellow), BIAS (blue), and FAR (green). The three distinct RI thresholds (i.e., 25, 30, and 35 knots) are shown separately in this figure.

found in Supporting Information S1 (Text S2; Figures S5 and S6). The TCs from the period 2010–2019 (i.e., 10 years) were validated separately over the NA. We verified a total of 168 TCs from this 10-year period.

Moreover, a contingency table (Table S1 in Supporting Information S1; Wilks, 2006) was used to carry out dichotomous (i.e., "yes" or "no") forecasts. We used four scores to evaluate the performance of the prediction, as follows:

$$\text{Accuracy} = \frac{\text{hits} + \text{correct negatives}}{\text{total}} \ (\text{Range}: 0 \text{ to } 1;\ \text{Perfect score}: 1) \quad (2)$$

$$\text{POD} = \frac{\text{hits}}{\text{hits} + \text{misses}} \ (\text{Range}: 0 \text{ to } 1;\ \text{Perfect score}: 1) \quad (3)$$

$$\text{BIAS} = \frac{\text{hits} + \text{false alarms}}{\text{hits} + \text{misses}} \ (\text{Range}: 0 \text{ to } \infty;\ \text{Perfect score}: 1) \quad (4)$$

$$\text{FAR} = \frac{\text{false alarms}}{\text{hits} + \text{false alarms}} \ (\text{Range}: 0 \text{ to } 1;\ \text{Perfect score}: 0) \quad (5)$$

The "Accuracy" term is used to assess the overall prediction performance of the RIWI, and the "probability of detection" (POD) indicates the fraction of observed events that were correctly forecasted. The "bias score" (BIAS) compares the frequency of forecast events with the frequency of observed events, which indicates whether the forecast system tends to under-forecast (BIAS <1) or over-forecast (BIAS >1) events. The "false alarm ratio" (FAR) is sensitive to false alarms and is a useful complement to the POD. The thresholds derived from Figure 2 were used to predict whether RI will occur during the lifetime of a TC. As shown in Figure 3, similar results were obtained for all three RI thresholds. The forecasting accuracy was ~80% and the BIAS was always close to 1, indicating an overall high prediction skill. About 30% of the RI warnings were incorrectly issued and about 60% of the RI events were correctly forecast. The performance of the RIWI was better than the National Hurricane Center (NHC) official forecasts, which have had a POD of <40% over recent years (Cangialosi et al., 2020).

4. Case Study: Hurricane Ida (2021)

To gain insight into how the RIWI would perform in an operational environment, the flow chart and an example for operational applications are shown in Figure 4. The whole process is kind like "wait for trigger" action. Instead of using all data before T_E all at once, these data are gradually used to construct RIWI along with the time because a real-time forecast is needed for operational application. The input data increases gradually with time, and the RIWI is recalculated after each moment of data update. Once the value of RIWI exceeds the threshold, this system will issue a RI warning. In addition, a case study was used to determine how many days in advance the warning could be issued.

The storm considered in this paper is the Category 4 Atlantic Hurricane Ida (2021), which was the second-most damaging and intense hurricane on record to make landfall in the U.S. state of Louisiana. After formation, it developed slowly for 60 hr and then experienced RI from the 18:00 UTC 26 August 2021 (Figure S7 in Supporting Information S1). The RIWI was calculated using the GFS-FNL data set from 00:00 UTC 25 August to 18:00 UTC 26 August (Figure S8 in Supporting Information S1). Although the GFS-FNL data set typically underestimates TC intensity, it is still close to the observational data for the period before RI, which allows it to be used to construct the RIWI (Figure S7 in Supporting Information S1). The RIWI threshold used above was also applied to this storm to determine whether RI would develop. For comparison purposes, we also used the RII (Kaplan & DeMaria, 2003; Kaplan et al., 2010) for probabilistic prediction during the same period. Our results show that an RI warning can be issued at a lead time of ~30 hr by using the RIWI (Figure 4), while there is no prediction skill for RII before the onset of RI. In fact, a good probability forecast for RI was found at 18:00 UTC 27 August

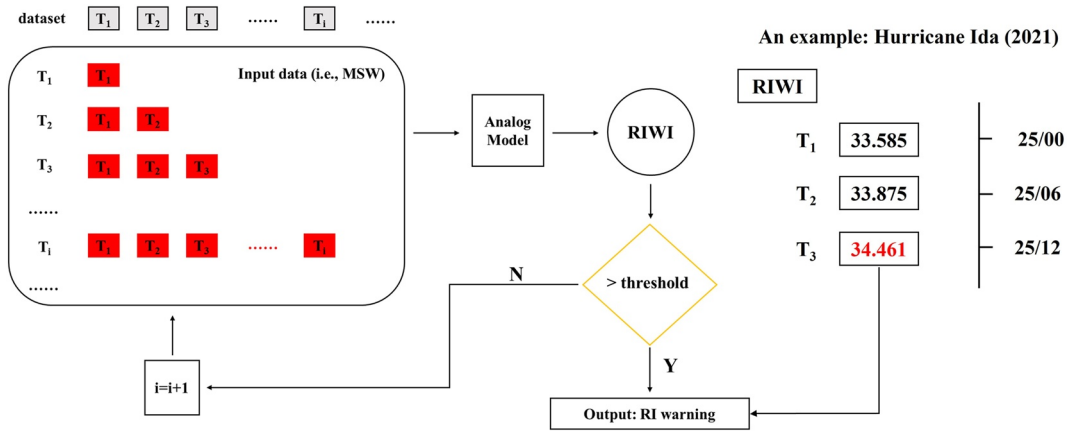

Figure 4. The flow chart and an example for operational applications. Left part of this figure shows the flow chart for operational applications: the input data (i.e., MSW) increases gradually with time; the output of the analog model is the RIWI. If the RIWI is less than the threshold, the system will wait for the next time and repeat this procedure; if the RIWI is greater than the threshold, an early RI warning could be issued. Right part of this figure shows an example for operational applications: the RIWI was recalculated at every 6 hours. At 12:00 UTC 25 August, the RIWI was greater than the threshold value and an early RI warning was issued.

(75.7%; not shown), by which time the TC had experienced RI for 24 hr. Hence, although the RI timing cannot be determined using the RIWI, the RIWI offers a considerable advantage over the RII approach with respect to issuing early RI warnings.

As an important statistic of TC intensification, an early estimate of the LMI can provide a direct sense of the severity of a TC. The LMI prediction for Hurricane Ida was obtained using the regression model constructed in Section 3.2. We found that the maximum forecast value of the LMI was 70 knots until RI onset, which differs significantly from the observational LMI (130 knots). As a super hurricane, its intensity variations were controlled not only by the environmental conditions, but also by the small-scale perturbations of the inner-core processes (Feng & Wang, 2021; Onderlinde & Nolan, 2016). However, the RIWI contains information related only to the early stage of TCs, leading to a lack of ability to capture the rapid development of small-scale convective processes during the RI period. Therefore, the prediction skill for LMI when using the RIWI is limited. We further found that a better relationship exists between the RIWI and LMI when Category 4 and 5 TCs were excluded. Consequently, we also constructed a regression model that excluded the Category 4 and 5 TCs. The root-mean-squared error (RMSE) was used to evaluate the performance of these models and of those that included all TCs during the period from 2010 to 2019. The results show that the forecasting error for TCs excluding Categories 4 and 5 is smaller than that when all TCs are included, which indicates that the RIWI would perform better when forecasting the LMI of a non-super hurricane (Figure S9 in Supporting Information S1). In addition, on average, even considering all storms, the RMSE of LMI forecasting for these hurricanes was still less than 30 knots, which could provide an early estimate of TC severity.

5. Discussion and Conclusions

In this study, an RIWI was developed using the local dynamical analog method. The RIWIs of all recorded TCs in the NA Basin were calculated and their forecast performance was verified using a 10-year cross-validation. We identified two features of the RIWI: (a) the RIWI can efficiently distinguish between RI and non-RI storms and an appropriate RIWI threshold can effectively predict the likelihood of RI; and (b) a significant positive correlation exists between the RIWI and LMI, indicating that the RIWI can be used as a predictor for forecasting the LMI. In addition, the potential application of the RIWI in an operational environment was further explored using the case study of Hurricane Ida (2021). Our results showed that an early warning can be issued ~30 hr before the onset of RI.

Both the length and quality of the sample data are important for the analog model constructing. It can be noted that the observational data used in this paper was a surprisingly long period for intensity studies (1851–2019). In fact, more accurate TC intensity estimations could be obtained since satellite measurements were developed (the

1960s; Hubert & Timchalk, 1969). The Figure S10 in Supporting Information S1 shows the RIWI constructed based on the data during the period of 1970–2019. Smaller shadow regions and larger difference between two CDF lines indicate that the data in this period indeed improves the performance of the RIWI to distinguish between RI storms and non-RI storms. However, what has to be admitted is that the analogous events for storms were also decreasing sharply because of the limited time. On average, only 45% analogous events could be found for a storm against to the period of 1851–2019. Taking the Hurricane Ida as an example, when the period of 1970–2019 is used, none of analogous event could be found before RI timing. Hence, longer, high-quality data will be needed to improve the performance of the analog model in the future. Another important point to be considered is the possibility of improving the RIWI by incorporating additional variables. The potential and stability of the RIWI also needs to be explored further in more operational forecasting scenarios.

Data Availability Statement

The IBTrACS data set is available at https://www.ncdc.noaa.gov/ibtracs/, and the GFS-FNL data set is available at https://rda.ucar.edu/datasets/ds083.2/. The RII is available from the NHC (https://ftp.nhc.noaa.gov/atcf/stext/). The index constructing and other data processing were performed using NCAR Command Language (NCL) and Bash Shell, available at https://zenodo.org/record/7467091.

Acknowledgments
This work was supported by the National Natural Science Foundation of China (Grants 42105059 and 42225501).

References

Blake, E. S., Cangialosi, J. P., & Klotzbach, P. J. (2016). Is NHC intensity forecast skill increasing? In *32nd conference on hurricanes and tropical meteorology, San Juan, Puerto Rico*. American Meteorological Society. Retrieved from https://ams.confex.com/ams/32Hurr/webprogram/Paper293532.html

Cangialosi, J. P., Blake, E., DeMaria, M., Penny, A., Latto, A., Rappaport, E., & Tallapragada, V. (2020). Recent progress in tropical cyclone intensity forecasting at the National Hurricane Center. *Weather and Forecasting*, *35*(5), 1913–1922. https://doi.org/10.1175/WAF-D-20-0059.1

Chen, Y., & Wu, C. (2022). On the two types of tropical cyclone eye formation: Clearing formation and banding formation. *Monthly Weather Review*, *150*(6), 1457–1473. https://doi.org/10.1175/mwr-d-21-0239.1

DeMaria, M., & Kaplan, J. (1994). Sea surface temperature and the maximum intensity of Atlantic tropical cyclones. *Journal of Climate*, *7*(9), 1324–1334. https://doi.org/10.1175/1520-0442(1994)007,1324:SSTATM.2.0.CO;2

Ding, R. Q., Li, J., & Seo, K. (2011). Estimate of the predictability of boreal summer and winter intraseasonal oscillations from observations. *Monthly Weather Review*, *139*(8), 2421–2438. https://doi.org/10.1175/2011MWR3571.1

Ding, R. Q., Li, J. P., & Seo, K.-H. (2010). Predictability of the Madden–Julian oscillation estimated using observational data. *Monthly Weather Review*, *138*(3), 1004–1013. https://doi.org/10.1175/2009mwr3082.1

Emanuel, K. (2000). A statistical analysis of tropical cyclone intensity. *Monthly Weather Review*, *128*(4), 1139–1152. https://doi.org/10.1175/1520-0493(2000)128<1139:asaotc>2.0.co;2

Emanuel, K., & Zhang, F. (2016). On the predictability and error sources of tropical cyclone intensity forecasts. *Journal of the Atmospheric Sciences*, *73*(9), 3739–3747. https://doi.org/10.1175/JAS-D-16-0100.1

Emanuel, K. A. (2005). Increasing destructiveness of tropical cyclones over the past 30 years. *Nature*, *436*(7051), 686–688. https://doi.org/10.1038/nature03906

Feng, J., & Wang, X. G. (2019). Impact of assimilating upper-level dropsonde observations collected during the TCI field campaign on the prediction of intensity and structure of Hurricane Patricia (2015). *Monthly Weather Review*, *147*(8), 3069–3089. https://doi.org/10.1175/mwr-d-18-0305.1

Feng, J., & Wang, X. G. (2021). Impact of increasing horizontal and vertical resolution of the hurricane WRF model on the analysis and prediction of Hurricane Patricia (2015). *Monthly Weather Review*, *149*(2), 419–441. https://doi.org/10.1175/MWR-D-20-0144.1

Gall, R., Franklin, J., Marks, F., Rappaport, E. N., & Toepfer, F. (2013). The hurricane forecast improvement project. *Bulletin of the American Meteorological Society*, *94*(3), 329–343. https://doi.org/10.1175/BAMS-D-12-00071.1

Hou, Z., Zuo, B., Zhang, S., Huang, F., Ding, R., Duan, W., & Li, J. (2020). Model forecast error correction based on the local dynamical analog method: An example application to the ENSO forecast by an intermediate coupled model. *Geophysical Research Letters*, *47*(19), e2020GL088986. https://doi.org/10.1029/2020GL088986

Hubert, L. F., & Timchalk, A. (1969). Estimating hurricane wind speeds from satellite pictures. *Monthly Weather Review*, *97*(5), 382–383. https://doi.org/10.1175/1520-0493(1969)097<0382:ehwsfs>2.3.co;2

Judt, F., & Chen, S. S. (2016). Predictability and dynamics of tropical cyclone rapid intensification deduced from high-resolution stochastic ensembles. *Monthly Weather Review*, *144*(11), 4395–4420. https://doi.org/10.1175/MWR-D-15-0413.1

Kaplan, J., & DeMaria, M. (2003). Large-scale characteristics of rapidly intensifying tropical cyclones in the North Atlantic basin. *Weather and Forecasting*, *18*(6), 1093–1108. https://doi.org/10.1175/1520-0434(2003)018<1093:LCORIT>2.0.CO;2

Kaplan, J., DeMaria, M., & Knaff, J. A. (2010). A revised tropical cyclone rapid intensification index for the Atlantic and eastern North Pacific basins. *Weather and Forecasting*, *25*(1), 220–241. https://doi.org/10.1175/2009WAF2222280.1

Kaplan, J., Rozoff, C. M., DeMaria, M., Sampson, C. R., Kossin, J. P., Velden, C. S., et al. (2015). Evaluating environmental impacts on tropical cyclone rapid intensification predictability utilizing statistical models. *Weather and Forecasting*, *30*(5), 1374–1396. https://doi.org/10.1175/WAF-D-15-0032.1

Knapp, K. R., Diamond, H. J., Kossin, J. P., Kruk, M. C., & Schreck, C. J. (2018). *International Best Track Archive for Climate Stewardship (IBTrACS) Project, version 4*. [indicate subset used]. NOAA National Centers for Environmental Information. https://doi.org/10.25921/82ty-9e16

Knapp, K. R., Kruk, M. C., Levinson, D. H., Diamond, H. J., & Neumann, C. J. (2010). The International Best Track Archive for Climate Stewardship (IBTrACS): Unifying tropical cyclone best track data. *Bulletin of the American Meteorological Society*, *91*(3), 363–376. https://doi.org/10.1175/2009BAMS2755.1

Kossin, J. P., Emanuel, K., & Vecchi, G. (2014). The poleward migration of the location of tropical cyclone maximum intensity. *Nature*, *509*(7500), 349–352. https://doi.org/10.1038/nature13278

Landsea, C. W., & Franklin, J. L. (2013). Atlantic Hurricane database uncertainty and presentation of a new database format. *Monthly Weather Review*, *141*(10), 3576–3592. https://doi.org/10.1175/mwr-d-12-00254.1

Lee, C.-Y., Tippett, M. K., Sobel, A. H., & Camargo, S. J. (2016). Rapid intensification and the bimodal distribution of tropical cyclone intensity. *Nature Communications*, *7*(1), 10625. https://doi.org/10.1038/ncomms10625

Lewis, W. E., Rozoff, C., Alessandrini, S., & Delle Monache, L. (2020). Performance of the HWRF Rapid Intensification Analog Ensemble (HWRF RI-AnEn) during the 2017 and 2018 HFIP real-time demonstrations. *Weather and Forecasting*, *35*(3), 841–856. https://doi.org/10.1175/WAF-D-19-0037.1

Li, J., & Ding, R. (2011). Temporal–spatial distribution of atmospheric predictability limit by local dynamical analogues. *Monthly Weather Review*, *139*(10), 3265–3283. https://doi.org/10.1175/MWR-D-10-05020.1

Lorenz, E. N. (1969). The predictability of a flow which possesses many scales of motion. *Tellus*, *21*(3), 289–307. https://doi.org/10.1111/j.2153-3490.1969.tb00444.x

Needham, H. F., Keim, B. D., & Sathiaraj, D. (2015). A review of tropical cyclone-generated storm surges: Global data sources, observations, and impacts. *Reviews of Geophysics*, *53*(2), 545–591. https://doi.org/10.1002/2014RG000477

Onderlinde, M., & Nolan, D. (2016). Tropical cyclone-relative helicity and the pathways to intensification in shear. *Journal of the Atmospheric Sciences*, *73*(2), 869–890. https://doi.org/10.1175/jas-d-15-0261.1

Shu, S., Ming, J., & Chi, P. (2012). Large-scale characteristics and probability of rapidly intensifying tropical cyclones in the western North Pacific Basin. *Weather and Forecasting*, *27*(2), 411–423. https://doi.org/10.1175/WAF-D-11-00042.1

Tsai, H., & Elsberry, R. L. (2019). Combined three-stage 7-day weighted analog intensity prediction technique for western North Pacific tropical cyclones: Demonstration of optimum performance. *Weather and Forecasting*, *34*(6), 1979–1998. https://doi.org/10.1175/waf-d-19-0130.1

Wilks, D. S. (2006). *Statistical methods in the atmospheric sciences* (2nd ed., p. 627). Academic Press.

Zhang, F., & Sippel, J. A. (2009). Effects of moist convection on hurricane predictability. *Journal of the Atmospheric Sciences*, *66*(7), 1944–1961. https://doi.org/10.1175/2009JAS2824.1

Zhang, F., & Tao, D. (2013). Effects of vertical wind shear on the predictability of tropical cyclones. *Journal of the Atmospheric Sciences*, *70*(3), 975–983. https://doi.org/10.1175/jas-d-12-0133.1

Zhong, Q., Li, J., Zhang, L., Ding, R., & Li, B. (2018). Predictability of tropical cyclone intensity over the western North Pacific using the IBTrACS dataset. *Monthly Weather Review*, *146*(9), 2741–2755. https://doi.org/10.1175/mwr-d-17-0301.1

Zhong, Q., Zhang, L., Li, J., Ding, R., & Feng, J. (2018). Estimating the predictability limit of tropical cyclone tracks over the western North Pacific using observational data. *Advances in Atmospheric Sciences*, *35*(12), 1491–1504. https://doi.org/10.1007/s00376-018-8008-7